Developing Hull Design Based on the Hydrodynamic Criteria: An Application for Leisure Boats as a Tourist Facility

Ahmad Ramadhan Yusfianda [1], Hananta Diatmaja [1], Aditya Rio Prabowo [1,*], Tuswan Tuswan [2,*], Teguh Muttaqie [3], Nurul Muhayat [1], Joung Hyung Cho [4], Wibowo Wibowo [1], and Emel Mixsa Muslimy [5]

[1] Department of Mechanical Engineering, Universitas Sebelas Maret, Surakarta, Indonesia
[2] Department of Naval Architecture, Universitas Diponegoro, Semarang, Indonesia
[3] Research Center for Testing Technology and Standards, National Research and Innovation Agency (BRIN), Tangerang, Indonesia
[4] Department of Industrial Design, Pukyong National University, Busan, South Korea
[5] P.T. Marathon Pacific Marines, Tangerang, Indonesia
Email: yusfianda@student.uns.ac.id (A.R.Y.); hananta037@student.uns.ac.id (H.D.); aditya@ft.uns.ac.id (A.R.P.); tuswan@lecturer.undip.ac.id (T.T.); teguh.muttaqie@brin.go.id (T.M.); nurulmuhayat@staff.uns.ac.id (N.M.); jhcho7@pknu.ac.kr (J.H.C.); wibowo69@staff.uns.ac.id (W.W.); emixsa19@gmail.com (E.M.M.)
*Corresponding author

***Abstract*—The tourism sector plays a vital role in the Indonesian economy. Indonesia's mainstay tourism sector is coastal tourism. Biodiversity and marine wealth in coastal areas are essential potentials to support sustainable development in Indonesia. For example, the Raja Ampat Islands have made tourism a leading sector for sustainable development. Currently, transportation in Indonesian maritime tourism is still dominated by ships with traditional hull models with poor hydrodynamic performance. Therefore, it is necessary to update the leisure boat model to have better hydrodynamic performance so that tourists can travel more safely and comfortably. In this study, an update of the leisure boat hull model was carried out by conducting a hydrodynamic analysis on five reference ships with Length Overalls (LOAs) of 6–8 m. After, the dimensions were processed with the regression method to obtain the proposed ship dimensions with three boat hull variation models and three dimensions variations. Following this, the hydrodynamic characteristics of each ship were analyzed using regression sensitivity to find the effect of each model variation, so it can help give further consideration while designing the ship. Each model analyzed was given points to obtain the best results with the Multiattribute Decision-Making (MADM) method. The results of this study found that making a hull model using the regression method with the deep vee model with dimension variation 1 had the best hydrodynamic characteristics. The results of this study are also expected to give reference and help consider the design of leisure boat hull models.**

***Keywords*—archipelagic country, leisure boat, design method, hydrodynamic**

I. Introduction

Approximately 66% of Indonesia's land comprises vast oceans, encompassing a coastline that extends 54,716 km in total. Positioned strategically between the continents of Asia and Australia and bordered by the Indian Ocean and the Pacific Ocean, Indonesia holds the promising prospect of becoming a global maritime center [1]. The vast area of water owned by Indonesia also causes Indonesia to have extensive aquatic tourism potential, much of which has not been explored. The tourism sector is industry-oriented toward people and their active participation in various fields of activity in the tourism sector [2]. Tourism plays a vital role in the Indonesian economy as a source of foreign exchange earnings and by creating employment and business opportunities [3]. Indonesia's mainstay tourism sector is coastal tourism. The diverse biodiversity and marine wealth in coastal areas have significant potential to support sustainable development in Indonesia [4]. For example, the Raja Ampat Islands have made tourism a leading sector for sustainable development [5].

Raja Ampat is a marine conservation area consisting of 4.6 million hectares of ocean and 1,411 small islands, coral reefs, and atolls surrounding four main islands: Waigeo, Batanta, Salawati, and Misoo [6]. Raja Ampat is famous for its diving spots, which are the main attraction for tourists. The condition of the coral reefs and the fish species are the main tourist attractions, as seen in Fig. 1 [7]. However, it is crucial to manage tourism sustainably to protect the marine environment and ensure that it remains a beautiful and healthy ecosystem to fulfill Sustainable Development Goals (SDGs).

Manuscript received September 12, 2023; revised November 6, 2023; accepted November 22, 2023; published June 6, 2024.

The large number of unexplored marine areas for tourism shows that the tourism sector in Indonesia can still be developed further. It is necessary to explore new areas of marine tourism and advanced infrastructure for water tourism so that tourists are safe and comfortable when traveling. This will attract higher interest from tourists to form sustainable tourism. Sustainable tourism involves elements of ecological sustainability, social acceptability, cultural adaptability, and economic viability, so it can help actualize SDGs [8].

Fig. 1. Raja Ampat water tourism area [9].

Past research endeavors in ship hull studies primarily examined how hull appendages influenced drag coefficients [10–12]. Variations in the Earth's climate impact the properties of ocean water, consequently, influencing a ship's hydrodynamic performance. Therefore, it becomes imperative to carefully observe a ship's behavior under specific conditions [13]. Researchers have optimized hulls to determine efficient shapes and good hydrodynamic performance [14–16]. On the other hand, no one has conducted more profound research to determine the magnitude of the effect of dimensional changes and changes in the type of hull used.

To determine a ship's main dimensions and appropriate hull shape, it is necessary to develop an efficient method. One strategy that can be used is the regression approach method, because it can achieve a similarity of 99.474% with its reference [17]. In ship design, the main characteristics that need to be determined are Length (L), Width (B), Draft (d), and Deadweight Tonnage (DWT) [18]. To achieve this, a regression analysis of the reference data is required [19–21]. In advancing the aquatic tourism sector in Indonesia, it is necessary to conduct further studies on efficient methods to develop leisure boats that meet the required criteria.

This study employed the regression analysis method to assess the performance criteria of resistance, stability, and seakeeping using an original vessel, or reference design, as a basis for evaluation. To achieve a hull that has an optimal efficiency for leisure boats, the Savitsky method was used for the resistance analysis, large angle stability for the stability analysis, and strip theory for the seakeeping analysis. Furthermore, the regression sensitivity method was used to determine the effect of each type of hull model variation and dimensions used, so it can give further consideration while determining the dimensions and type of hull used in designing leisure boats and other types of ships according to their operational needs. Subsequently, the models were subjected to the Multiattribute Decision-Making (MADM) method to identify the most appropriate design option based on the specified criteria. This investigation focused solely on hydrodynamic characteristics and omitted considerations of propulsion systems and hull construction types.

II. Literature Review

A. Design Method

Regression analysis is a statistical method to assess the causal relationship between one variable and another [18]. The causal variable is often described as variable *X* (i.e., independent variable), while the effect variable is defined as variable *Y* (i.e., dependent variable). This analysis method is one of the most widely used in machine learning. In ship design, this regression method is used to find the primary dimensions of the ship by looking at the relationships among the Ship Length (*LOA*), Ship Width (*B*), Ship Depth (*D*), and Ship Weight (i.e., displacement) [22]. Linear regression is a regression method, and the relationships among a ship's main dimensions (*LOA, B, D*, and *displacement*) in linear regression follow a regular, straight line. The mathematical model for linear regression is shown in Eq. (1).

$$Y = aX + b \tag{1}$$

where *Y* and *X* are variables, and *a* and *b* are constants.

B. Resistance Calculation

Resistance is one of the hydrodynamic parameters on the hull. In designing a ship, predicting resistance value is one of the critical factors [23]. Many types of resistance include friction, wave generation, and hull-shape drag. It is influenced by several factors, such as ship speed (V_s), ship weight, and hull shape [24]. Ship resistance has several supporting components, including wave, viscosity, and friction resistance. The total resistance of a ship can be seen in Eq. (2) and Fig. 2.

$$R_T = R_F + R_v + R_W \tag{2}$$

where R_T is total resistance, R_V is viscous resistance, dan R_W is wave resistance.

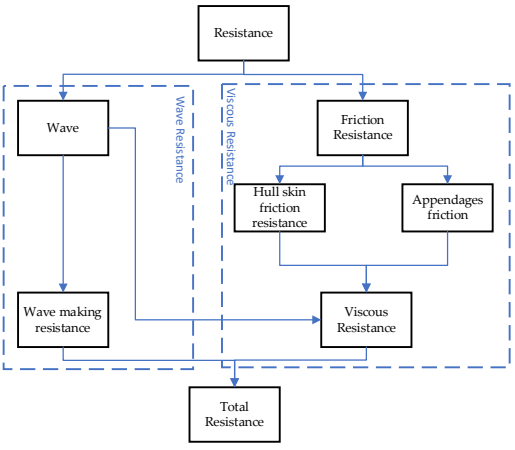

Fig. 2. Resistance type on the ship.

C. Savitsky Method

The Savitsky method constitutes a numerical approach employed in hydrodynamic calculations to estimate hull drag, wetted surface, center of pressure, drag, and resistance. Additionally, it can anticipate the speed, trim, deadrise angle, and load parameters [25]. For this reason, the formulas used in this study were based on the Savitsky method. The first assumption is that the planning hull is in a steady-state condition, implying no acceleration in any direction [26–29]. The formulas used in the Savitsky method can be seen in Eqs. (7) and (8).

$$D_f = \frac{c_f \rho {V_1}^2 (\lambda b^2)}{2 \cos \beta} \tag{7}$$

$$D = \Delta \tan \tau + \frac{D_f}{\cos \tau} \tag{8}$$

where D_f is drag friction, l is the mean value of the wet area's length-to-width ratio, b is the average chine beam of the planning vessel, β is the deadrise angle of the planning ship hull, Δ is the displacement, τ is the trim angle of the ship hull, and D is the total drag.

D. Holtrop Method

The Holtrop method is widely used to estimate the resistance and powering of displacement-type ships [30]. This method is only appropriate if the parameters used follow the modeling. Therefore, an expansion was carried out using a low L/B ratio, adjusting the submerged transom stem. The prediction formula is presented in Eq. (9) for the hull form factor [11].

$$1 + k_1 = c_{13}\left\{0.93 + c_{12}\left({B}/{L_R}\right)^{0.92497}(0.95 - C_p)^{-0.521448}(1 - C_p + 0.0255\, lcb)^{0.6906}\right\} \tag{9}$$

Eq. (10) shows the determination of the addition of resistance [11].

$$R_{APP} = 0.5\, \rho\, V^2 S_{APP} (1 + K_2)_{eq} C_f \tag{10}$$

where ρ is the water density, V is the ship speed, S_{APP} is the wetted area of the appendage, $1 + K_2$ is the resistance factor of the appendage, C_f is the frictional resistance coefficient of the ship according to the ITTC-1957 formula.

E. Stability Calculation

Stability is an essential aspect of designing a ship. Stability is the ability of a boat to return to its original position when the ship receives actual force [31–33]. Several essential factors affect ship stability, including buoyancy, gravity, and metacentric points. The points that affect a ship's stability can be seen in Fig. 3.

A boat will tilt or lean when subjected to an external force [31]. This will cause a change in the ship's center of buoyancy so that the ship's tilt angle changes. Changing the angle of inclination of the boat will affect the point of force received by the boat, affecting the value of the righting lever curve (GZ). The righting lever curve (GZ) is the perpendicular distance between the lines of action of the forces that occur [33]. Righting lever (GZ) curves are used to determine the level of safety, as regulated by various guidelines, one of which is the International Maritime Organization (IMO) based on IMO HSC200 [34].

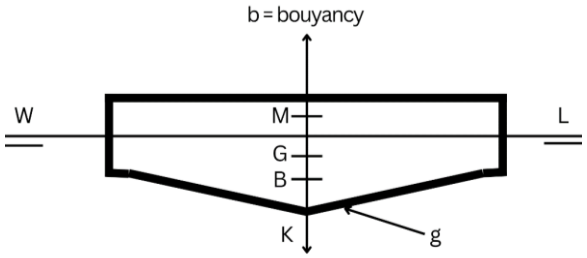

Fig. 3. Point of stability on the ship.

F. Seakeeping

Seakeeping is a vital element of ship design that enhances the efficiency of a vessel's performance. The seakeeping ability of a boat is used to determine a ship's performance in various water conditions [18, 35]. Excessive ship motion leads to heightened fatigue among onboard personnel, diminishing their work capacity, and it can also result in hull damage due to repetitive movements [18, 36]. Seakeeping performance is also affected by water-related environmental factors and sailing speed. When a ship encounters waves, the boat will undergo motion along six axes, encompassing heave, pitch, yaw, sway, surge, and roll, as seen in Fig. 4. Of these six directions, only three are commonly used as references when designing a ship: heaving, rolling, and pitching [18].

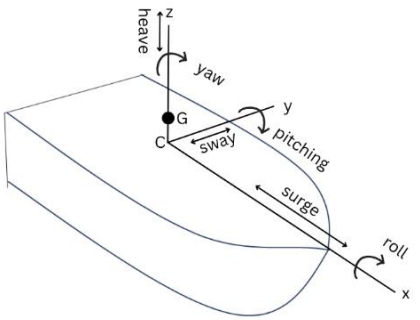

Fig. 4. Six degrees of freedom on a ship's hull.

Heaving is an up- and downwards movement parallel to the *z*-axis [18]. To determine the value of heaving, one can use Eq. (11).

$$a\ddot{z} + b\dot{z} + cz = F_0 Cos\omega_\theta t \tag{11}$$

where a$\ddot{z}$ is inertial force, b$\dot{z}$ is damping force, cz is restoring force, and $F_0 \mathrm{Cos}\omega_\theta t$ is the exciting force.

Rolling is the movement of a ship around the *x*-axis due to waves coming from the ship's side. Roll movement analysis uses the following Eq. (12).

$$a\frac{d^2\emptyset}{dt} + a\frac{d\emptyset}{dt} + c\emptyset = M_o cos\omega_\theta t \tag{12}$$

where $a\frac{d^2\emptyset}{dt}$ is inertial force, $a\frac{d\emptyset}{dt}$ is the damping force, $c\emptyset$ is the restoring force, and $M_o \cos\omega_\theta t$ is the exciting force.

Pitching is the motion of a vessel. This motion can occur because of waves that cause a height difference between a hull's front and back [37]. Eq. (13) is used to determine the heaving motion.

$$\mathrm{d}\ddot{\emptyset} + e\emptyset + h\emptyset = M_{0.}\mathrm{Cos}\omega_{\mathrm{e}}\mathrm{t} \quad (13)$$

where $d\ddot{\emptyset}$ is the inertial force, $e\emptyset$ is the damping force, $h\emptyset$ is the restoring force, and $M_{0.}\mathrm{Cos}\omega_{\mathrm{e}}\mathrm{t}$ is the exciting force.

G. Response Amplitude Operator

The Response Amplitude Operator (RAO), referred to as the transfer function, represents the relationship between the magnitude of a ship's response and the importance of ocean waves. It describes the transfer function resulting from waves striking the hull within a specific frequency range. Using numerical simulations, the RAO predicts a ship motions, including surge, sway, heave, roll, pitch, and yaw [38]. The equation for the RAO is specified as Eq. (14).

$$\mathrm{RAO} = \left(\frac{\emptyset_a}{\zeta_a}\right)^2 \quad (14)$$

where $\emptyset_a$ is the amplitude of ship motion response and ζ_a is the amplitude of the incident wave (deg).

H. Motion Sickness Incidance

One parameter for determining discomfort due to a ship's movement is Motion Sickness Incident (MSI). Motion sickness is distinguished by unpleasant physical sensations, like dizziness, nausea, paleness, breathing difficulties, and vomiting. It is commonly referred to as seasickness due to a ship's motion. [39]. The MSI index is employed to estimate the probability of seasickness, and its calculation involves Eq. (15) [40].

$$MSI = 100\left[0.5 + erf\left(\frac{log_{10}\,(0.798\sqrt{m_4}/g) - \mu_{MSI}}{0.4}\right)\right] \quad (15)$$

I. Deck Wetness

Deck wetness is the result of the rising of seawater onto the deck of a ship, which can cause damage and impact the comfort of the crew and passengers on board [41]. Deck wetness can occur because of waves or extreme ship movements. To determine the value of deck wetness, the following Eq. (16) can be used [40].

$$P(Deck\ wetness) = \exp\left(\frac{-fe^2}{2m_0}\right) \quad (16)$$

where, m_0 is the relative vertical m otion spectrum and *fe* is the effective board.

J. Slamming

Slamming occurs when a ship hits ocean waves at highspeed resulting in enormous pressure on the hull. Slamming can cause damage to the hull and can impact the balance of the ship. Slamming can occur at the bottom of the boat or on the deck of the vessel. The equation to determine the slamming value can be seen in Eq. (17) as follows [40].

$$P(slamming) = exp\left(-\frac{d^2}{2m_0} - \frac{Vcr^2}{2m_2}\right) \quad (17)$$

where, m_2 is the relative vertical velocity spectrum, V_{cr} is the threshold velocity, and *d* is the draft.

K. Sensitivity Analysis

A sensitivity analysis is conducted to determine the effect of each variation that will be tested. In this analysis, variations were made to input values, and the impact on the output values was measured. The purpose of the regression sensitivity analysis was to determine how much influence each input variable had on the output variable to help in decision making and strategic planning.

The estimation result of a parameter is considered sensitive if a slight change in the parameter causes a drastic change in the value. Conversely, suppose the estimation results obtained are not significantly different because of parameter changes. In that case, it is said that the estimation results are relatively insensitive to the value of these parameters [41]. In conducting a sensitivity analysis, it should be noted that the results may vary depending on the model or system used and the range of values selected for each variable.

L. Multi-Attribute Decision Making

Multiattribute Decision Making (MADM) is an approach used to make decisions among various available alternatives based on a set of limited attributes or criteria [42]. The simple weighted addition method (SAW) is a type of MADM approach utilized for straightforward weighting, and its simplicity has made it widely favored among practitioners [43]. The basic concept of the SAW method is to find the weighted sum of performance ratings for each alternative of all attributes. The SAW method requires the normalization of the decision matrix (X) to a scale that can be compared with all existing alternative ratings. The definition of the normalization of the decision matrix can be found in Eq. (18). Afterward, the preference value for each alternative is computed using Eq. (19).

$$r_{ij} = \begin{cases} \frac{x_{ij}}{Max_i x_{ij}} \\ \frac{Min_i x_{ij}}{x_{ij}} \end{cases} \quad (18)$$

$$V_i = \sum_{j=1}^{n} w_i r_{ij} \quad (19)$$

where *V* is the preference value, *W* is the weight criterion, and *r* is the normalized alternative value.

M. Monohull Variation

Ships with monohull hull types have several variations of hull types according to their needs. The variations of hull types used include shallow vee, deep vee, and round bottom. The hull shape significantly influences the wave flow pattern and hydrodynamic characteristics of a ship [44]. Each hull type has its uses and advantages, as well as disadvantages. The shallow vee hull type is one type of hull that is included in the planning category. It is

shaped like the letter v from the rearview, and it has two sides at the bottom where there is a space in the center between the left and right surfaces. The shallow vee hull type is often used as a patrol boat, rescue ship, ambulance ship, offshore supply ship, leisure/recreation ship, and for sports competitions [45]. The deep vee is a variation of the hull type that has a similar shape to the shallow vee, but the deep vee has a higher deadrise angle (20°). This type of hull is usually used on fast boats. Round-bottom hulls suit ships with a lot of cargo and with low speeds. A round-bottom hull is included in the displacement hull types, where most of the hull is supported by buoyancy. A round-bottom hull has a shape like a semicircle and does not have a rough break like a v-hull. An illustration of the variations of the monohull hull types can be seen in Fig. 5.

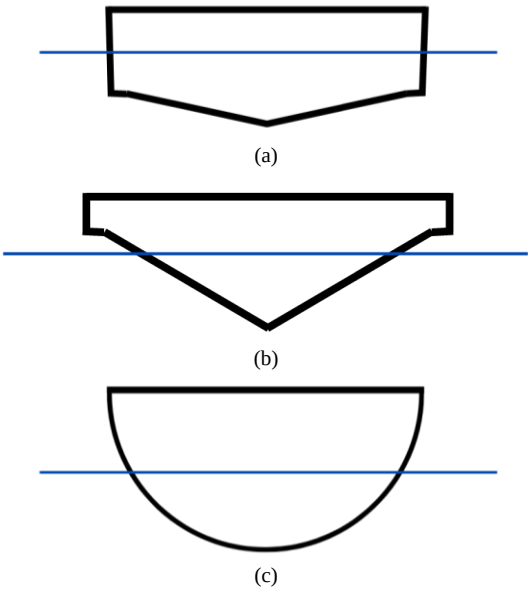

Fig. 5. Monohull type variations: (a) Shallow Vee; (b) Deep Vee; and (c) Round Bottom.

III. Methodology

The methodologies employed in this study included data collection, data processing, and data simulation. The data collection phase commenced with the identification of a reference leisure boat with a Length Overall (LOA) of 6–8 m. After the primary data of the reference ship were obtained, data processing was carried out using the regression approach method, because the regression method can produce similarities to a reference ship's main dimensions of 99.474% [18, 46]. A regression analysis was carried out to create three variations of the ship dimensions. Then, each variation of the dimensions was given four variations of the hull model, including a shallow vee, deep vee, and round bottom, which eventually produced nine hull variations. These obtained variations were simulated for hydrodynamic analysis, including resistance, stability, and seakeeping. After that, a regression sensitivity analysis was carried out to determine the effect of each variation tested. This study ignored the impact of the propulsion type and hull construction [47, 48]. The Multiattribute Decision-Making (MADM) method was used to determine the best leisure boat design. The results of this study are expected to provide an evaluation of leisure boat design methods based on their hydrodynamic characteristics [49–52]. A flowchart of this study can be seen in Fig. 6.

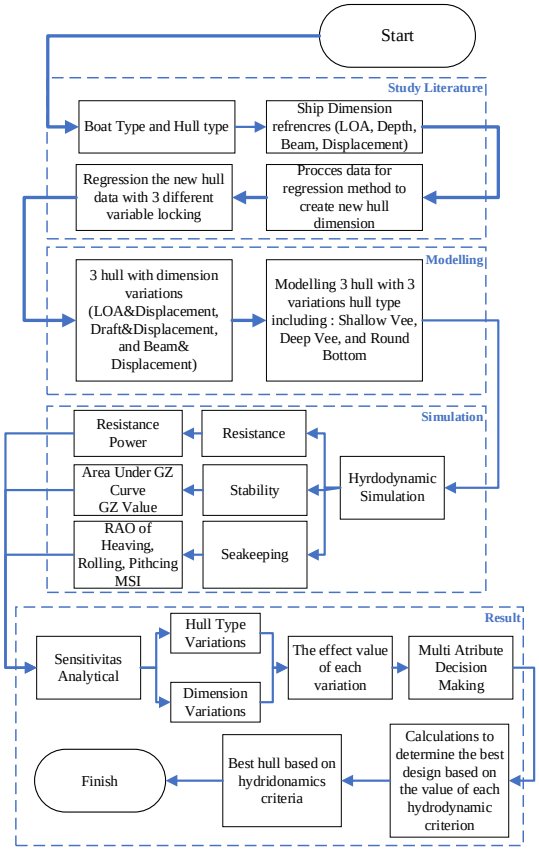

Fig. 6. Research method flowchart.

A. Data Collecting

In ship design, the hull shape is determined after the primary dimensions of the ship are established [18]. In this study, data collected from leisure boats with LOAs between 6 and 8 m were used as the basis for the reference vessel. Data on the primary dimensions of the selected reference vessels can be seen in Table I.

TABLE I. Reference Ship's Main Dimensions

Ship	LOA (m)	Beam (cm)	Depth (cm)	Draft (cm)	Displacement (ton)
Outborn Watercraft 7 m	7.00	2.29	1.10	0.30	0.95
FBI.0620.W A SB	6.00	2.00	1.00	0.40	1.80
6 m MBIG Speed Boat	6.00	2.10	1.00	0.35	1.80
7 m MBIG Speed Boat	7.03	2.30	1.50	0.40	2.20
8 m Sport Fishing JB	8.00	2.20	1.10	0.45	2.50

B. Designs Variations

After five reference vessels were determined, the primary dimensions for the new leisure boat design were determined using the regression approach method. This study used displacement as the independent variable and LOA, beam, and depth as the dependent variables. Charts of the regression results of the five reference vessels can be seen in Fig. 7.

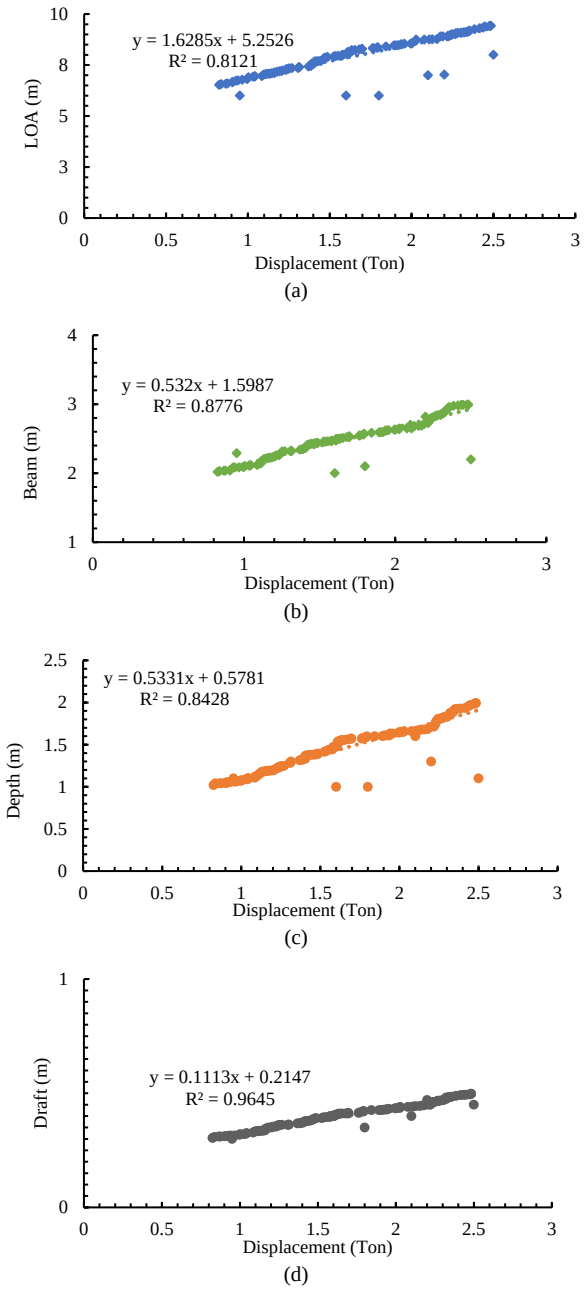

Fig. 7. Chart of regression result: (a) LOA vs. Displacement; (b) Beam vs. Displacement; (c) Depth vs. Displacement; and (d) Draft vs. Displacement.

Based on the linear regression results, as shown in Fig. 7, a linear equation was used to establish the dependent variable. This study used a target displacement of 1.68 tons, the average displacement of the five reference ships. Furthermore, calculations were carried out according to the resulting regression of the *y* value, and the target displacement was used according to the *x* value. The results of the primary dimensions calculation can be seen in Table II.

TABLE II. DIMENSION OF REGRESSION RESULT

Parameter	Value
LOA (m)	7.98
Beam (m)	2.49
Depth (m)	1.47
Displacement (ton)	1.68

This study analyzed the effect of the hydrodynamic characteristics of the hull on variations in the primary dimensions and hull type. Thus, it was necessary to conduct regression calculations again to obtain three dimensions variations. Three dimensions variations were obtained by locking three dependent variables: LOA and displacement, displacement and beam, and displacement and draft. One value of these sets of variables was a fixed variable, and the value of the other variable was a regression recalculation. The results of the regression calculations to obtain dimensions Variation 1 with locking LOA and displacement can be seen in Fig. 8 and the results of regression calculations for dimensions Variation 2 with locking depth and displacement in Fig. 9. Then, the results of the regression calculations for dimensions Variation 3 with the locking beam and displacement are presented in Fig. 10.

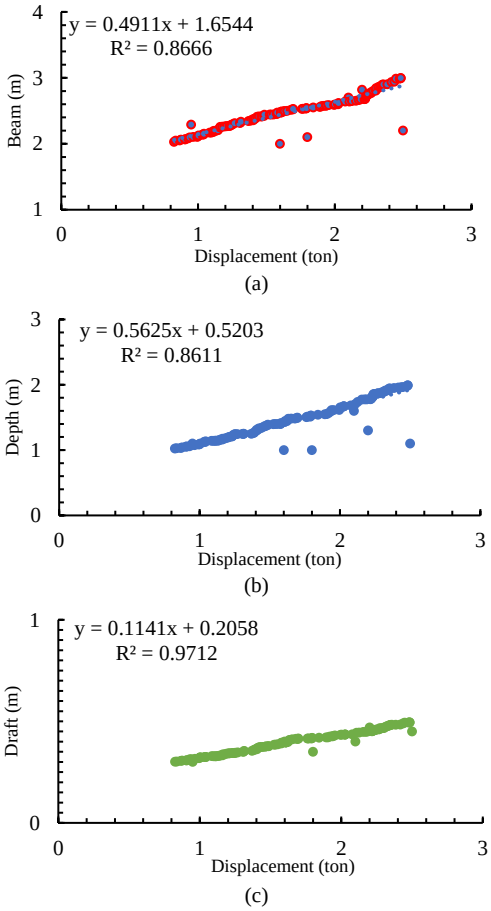

Fig. 8. Chart of regression result for the Variations 1 with locking LOA and Displacement: (a) Beam vs. Displacement; (b) Depth vs. Displacement; and (c) Draft vs. Displacement.

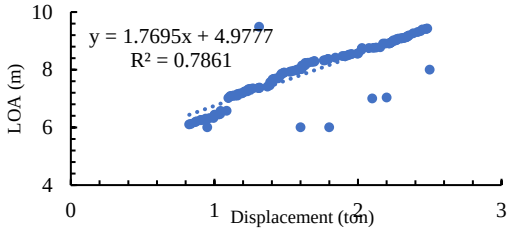

(a)

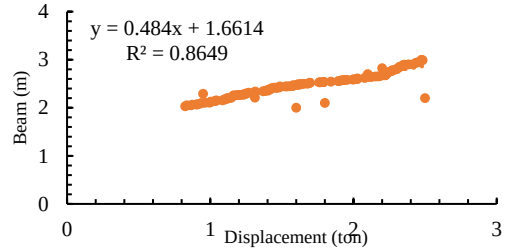

(b)

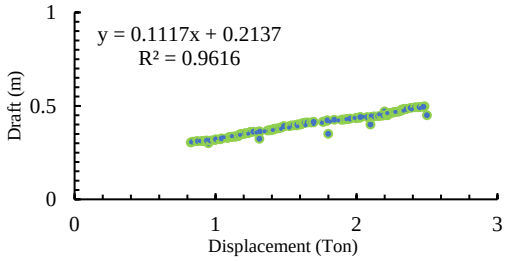

(c)

Fig. 9. Chart of regression result for the Variations 2 with locking Depth and Displacement: (a) LOA vs. Displacement; (b) Beam vs. Displacement; and (c) Draft vs. Displacement.

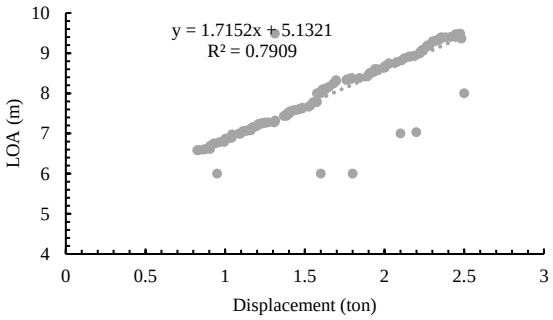

(a)

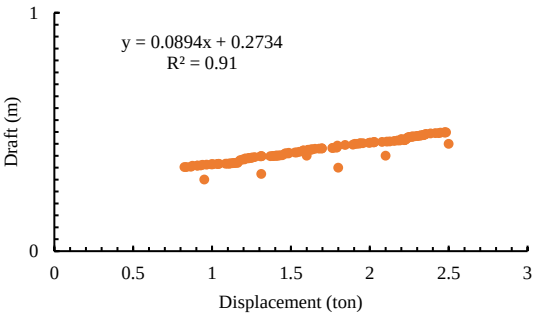

(b)

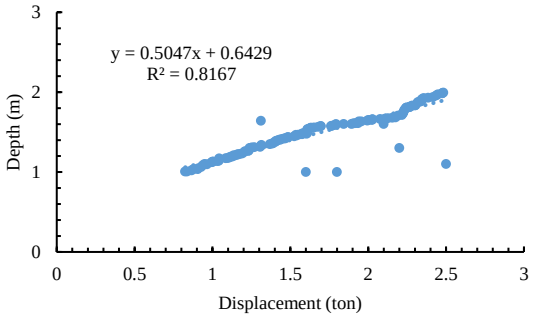

(c)

Fig. 10. Chart of regression result for the Variations 3 with locking Beam and Displacement: (a) LOA vs. Displacement; (b) Draft vs. Displacement; and (c) Depth vs. Displacement.

The results of the regression calculation produced three dimensions variations. Variation 1 is the result of the locking LOA and displacement data, Variation 2 is the result of the locking depth and displacement, and Variation 3 is the result of the locking beam and displacement. A recapitulation of the main dimensions calculation results with the dimensions variations can be seen in Table III.

TABLE III. RECAPITULATION VARIATIONS DIMENSION FROM THE REGRESSION METHOD

Parameter	Value		
	Variation 1	Variation 2	Variation 3
LOA (m)	7.98	8.01	7.94
Beam (m)	2.48	2.49	2.47
Depth (m)	1.46	1.49	1.40
Draft (m)	0.40	0.42	0.40
Displacement (ton)	1.68	1.68	1.69

After the dimensional data were obtained, the next step was to create a 3D hull model with Maxsurf Modeller to produce a line plan. This study also analyzed the hull type's effect on the ship's hydrodynamic character. Thus, each dimensions variation obtained was made into three types of hulls, namely, shallow vee, deep vee, and round bottom. The total number of models that were analyzed in this study is nine models. The 3D models with variations in hull shape can be seen in Fig. 11.

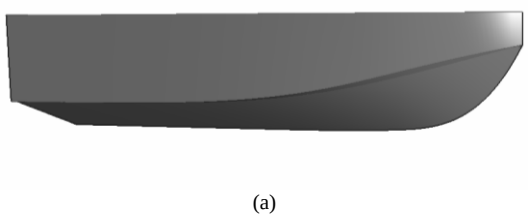

(a)

(b)

(c)

Fig. 11. 3D model hull with hull type variations: (a) Shallow Vee; (b) Deep Vee; and (c) Round Bottom.

C. Simulation Analysis

Once the 3D design process was finished, the subsequent step involved a simulation to evaluate the hydrodynamic attributes of each variation examined in this study. A recapitulation of the model can be seen in Table IV.

TABLE IV. MODEL RECAPITULATION

Model	LOA (m)	Beam (m)	Depth (m)	Draft (m)	Displacement (ton)
Shallow Vee 1	7.98	2.48	1.46	0.40	1.68
Shallow Vee 2	7.98	2.49	1.49	0.42	1.68
Shallow Vee 3	7.94	2.47	1.40	0.40	1.68
Deep Vee 1	7.98	2.48	1.46	0.40	1.68
Deep Vee 2	7.98	2.49	1.49	0.42	1.68
Deep Vee 3	7.94	2.47	1.40	0.40	1.68
Round Bottom 1	7.98	2.48	1.46	0.40	1.68
Round Bottom 2	7.98	2.49	1.49	0.42	1.68
Round Bottom 3	7.94	2.47	1.40	0.40	1.68

The simulations in this study included resistance, stability, and seakeeping. This study also considered environmental factors, and the simulations were carried out using parameters of the environmental conditions in the waters of Raja Ampat, Indonesia, which were taken based on seatemperatu.re website [53]. Water density data were taken from ITTC'57 based on the water temperature conditions. The environmental parameter factors in this study can be seen in Table V.

TABLE V. INFLUENCING ENVIRONMENT PARAMETERS

Parameter	Value	Units
Water Density	1021.76	kg/m^3
Windspeed	13.00	kts
Wave Height	0.80	m

The resistance simulation was carried out using Maxsurf Resistance with the Savitsky method to simulate the shallow vee model and deep vee model. The Holtrop method was used to simulate the round-bottom model. The resistance analysis was carried out in a speed range of 10–50 kts, producing the resistance value and power required for the ship to operate.

In the stability simulation, Maxsurf Stability was used to calculate the value of the stability of the ship. The simulation was conducted with a tilt angle between 0 and 180°. In the large angle stability analysis, the load case setting used was the free trim load case. The result of this simulation was the value of the stability when the ship was in a static condition with the value of the GZ arm.

The seakeeping simulation used Maxsurf Motions with the strip theory method. The hull was not meshed, but the hull was mapped into 41 sections prior to conducting the analysis. In this study, a wave direction variation of 90° (beam sea) and 180°. (head sea) was used with a sailing speed of 30 kts and a wave height of 0.8 m, which is the average wave height in the waters of Raja Ampat. The type of wave spectra used in this study were JONSWAP spectra. The results of the seakeeping simulation are displayed with RAO charts in heaving, rolling, and pitching movements, as well as charts of Motion Sickness Incidence (MSI), to determine the ship's motion response when crashing into waves and the level of seasickness in passengers on board when sailing.

IV. RESULTS AND DISCUSSION

Each design variation was simulated for resistance, stability, and seakeeping to determine the hydrodynamic characteristics of the hull. Data from the simulation results of each variation were compared based on the resistance, stability, and seakeeping values using regression sensitivity analysis to determine the effect of each given variation.

A. Resistance Simulation

This study conducted a resistance analysis with the nine hull variations based on the dimensions and hull model. The results of the resistance simulation on the variations with the regression method can be seen in Tables VI and VII.

Based on the data above, it was found that each variation of the same hull model with different dimensions variations had a resistance value that tended to be similar. Based on Table VII, the shallow vee hull-type variation was the hull model with the highest resistance value compared to the other models, with a value of 16.90 kN at 50 kts. Meanwhile, the deep vee hull model obtained the lowest resistance value of 8.70 kN at a speed of 50 kts.

TABLE VI. RESISTANCE RESULT OF THE NINE HULL VARIATIONS

Model		Speed (kts)				
		10	20	30	40	50
Resistance (kN)	Shallow Vee 1	1.40	4.30	7.70	11.70	16.20
	Shallow Vee 2	1.50	4.60	8.20	12.30	16.90
	Shallow Vee 3	1.40	4.50	7.90	12.00	16.50
	Deep Vee 1	0.80	2.10	3.90	6.10	8.70
	Deep Vee 2	0.80	2.30	4.10	6.40	9.20
	Deep Vee 3	0.80	2.20	4.00	6.30	9.00
	Round Bottom 1	1.40	3.00	5.80	9.30	13.60
	Round Bottom 2	1.40	3.10	6.00	9.60	14.00
	Round Bottom 3	1.40	3.00	5.80	9.40	13.60

TABLE VII. POWER PREDICTION RESULT OF THE NINE HULL VARIATIONS

Model		Speed (kts)				
		10	20	30	40	50
Power (eKW)	Shallow Vee 1	7.00	44.46	119.14	240.26	415.88
	Shallow Vee 2	7.48	47.71	126.26	252.48	434.20
	Shallow Vee 3	7.21	45.97	122.51	246.15	424.73
	Deep Vee 1	3.91	21.78	60.16	125.27	224.01
	Deep Vee 2	4.24	23.39	64.00	132.43	235.83
	Deep Vee 3	4.05	22.58	62.22	129.24	230.62
	Round Bottom 1	6.99	30.73	89.36	191.90	348.76
	Round Bottom 2	7.29	31.75	92.36	198.57	361.29
	Round Bottom 3	7.02	30.85	89.71	192.67	350.15

For the power value, a similar trend was obtained with the resistance value, where each variation of the same model with dimensions variations had results that tended to be similar. The shallow vee model variation still had the highest power value, with a value of 434.20 eKW at a speed of 50 kts. At the same time, the deep vee hull-type variation also occupied the lowest power value, achieving its highest power value of 224.01 eKW at a speed of 50 kts. Based on Table VII, it can also be concluded that the increasing importance of resistance was in line with the rising value of the power required

B. *Stability Simulation*

A ship's strength and stability can be used to obtain the stability value of a ship [18]. In this study, the stability value of the boat is displayed in the form of a GZ curve chart compared to the increase in the ship's tilt angle. The stability values of the nine hull variations can be seen in Table VIII, and a chart of the GZ value against the rise in the boat's tilt angle can be seen in Fig. 12.

The stability simulation results showed that the most considerable GZ arm value obtained was by the deep vee hull model with a value of 0.394 m, and the largest maximum tilt angle was obtained by the round-bottom hull model with a value of 67.30°. In the largest area, the highest value was received by the shallow vee model with a value of 19.07 (m·deg), and the largest angle of the vanishing point value was obtained by the round-bottom model with a value of 104.810°.

TABLE VIII STABILITY SIMULATION OF THE NINE HULL VARIATIONS

Ship	Righting Lever Curve			
	GZ Maximum (m)	α (deg.)	Area (m·deg)	Angle of Van. (deg)
Shallow Vee 1	0.272	57.3	18.20	95.190
Shallow Vee 2	0.290	55.5	19.10	94.472
Shallow Vee 3	0.291	55.5	19.07	94.430
Deep Vee 1	0.389	60.9	17.61	100.866
Deep Vee 2	0.394	60.0	18.67	100.182
Deep Vee 3	0.381	61.8	17.08	101.266
Round Bottom 1	0.361	67.3	12.54	106.709
Round Bottom 2	0.332	64.5	12.28	103.165
Round Bottom 3	0.340	66.4	10.93	104.810

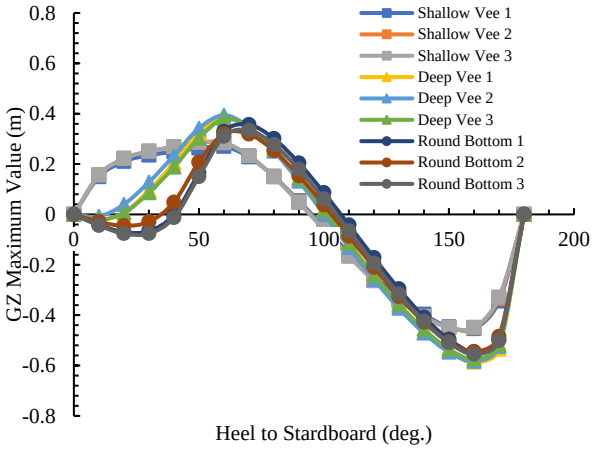

Fig. 12. Comparison of the GZ values with the ship's tilt of the nine hull variations.

C. *Seakeeping Simulation*

In this study, the seakeeping analysis was intended to determine the response of the ship's motion to the situation of the water's environment when the boat was in operation. The motion response of the boat was used to predict the ship's movement when the ship passes through waves so that the crew and passengers on board will remain safe and comfortable. In this study, several variations of wave directions were used, including 180°. (head sea), 135° (bow quarter sea), and 90°. (beam sea), with a constant speed of 30 kts. The seakeeping analysis produced RAO charts consisting of heaving, rolling, and pitching. The heaving RAO chart of the nine hull variations with 180°. wave direction can be seen in Fig. 13.

Based on the charts shown in Fig. 13, the boats with the shallow vee, deep vee, and round-bottom model variations had similar trend results during heaving motion. The maximum motion response was obtained on the ship with the round bottom 1 hull model variation at a frequency value of 4.82 rad/s during heaving motion compared to the other models. On the other hand, the slightest motion response was obtained in the shallow vee 1 hull model variation at a frequency value of 3.50 rad/s. It can be concluded that the round-bottom model has bad motion response during heaving movement compared to the other models.

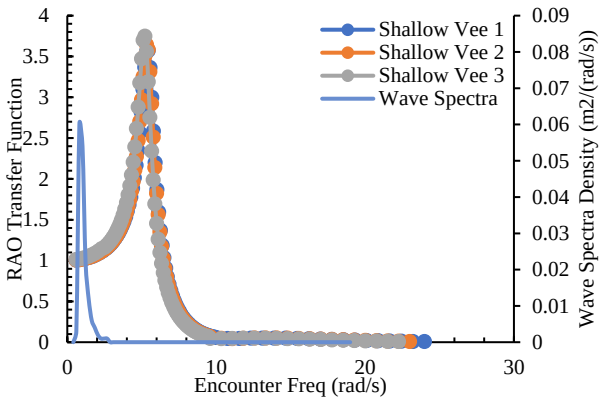

(a)

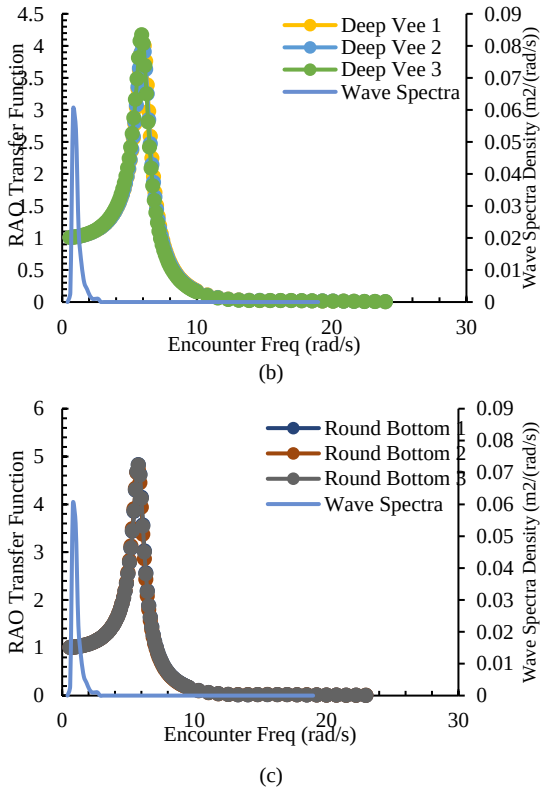

Fig. 13. RAO heaving motion, (a) shallow vee hull, (b) deep vee hull, (c) round bottom hull.

After analyzing the seakeeping during heaving motion, seakeeping during rolling motion was also examined. Rolling is movement to the right or left when a ship is sailing. This study used rolling motion when waves hit the boat from 90°. at a speed of 30 kts. The RAO charts of the rolling motion of the nine hull variations can be seen in Fig. 14.

Based on the data in the rolling RAO charts shown in Fig. 14, it was found that each variation of the ship model had a similar trend. In the shallow vee model, the highest motion response occurred at 3–4 rad/s frequencies, while in the other models, the highest motion response occurred at a frequency of 1–3 rad/s. For the deep vee 2 model, it obtained its highest motion response at a frequency of 1.93 rad/s. Conversely, the lowest movement response occurred in the round bottom 3 model at a frequency of 1.53 rad/s. Based on the RAO rolling charts of the nine hull variations, the waves did not experience superposition, which means that the ship did not receive more than one wave simultaneously, so the boat was more stable.

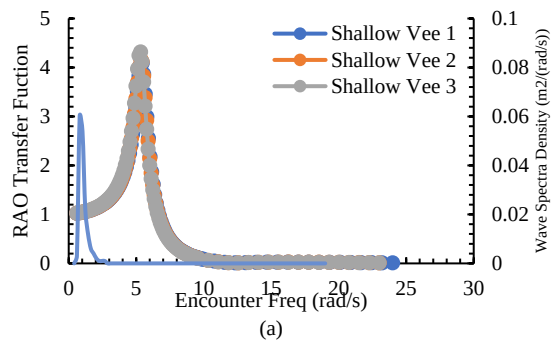

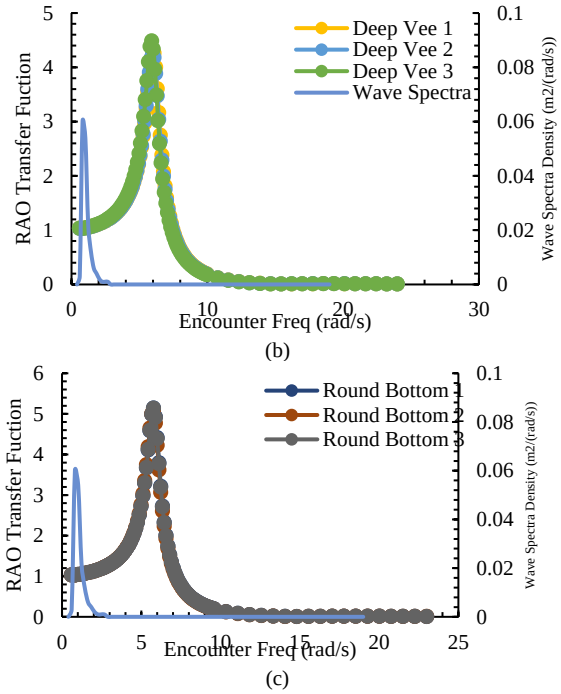

Fig. 14. RAO rolling motion, (a) shallow vee hull, (b) deep vee hull, (c) round bottom hull.

After analyzing seakeeping in the heaving and rolling movements, a seakeeping analysis was also carried out in the pitching movements. Pitching is the motion of a ship around the *y*-axis. When pitching motion occurs, the bow and stern alternately experience a change in trim. This study performed pitching motion when waves hit the ship from 180° at a speed of 30 kts. The RAO charts of the pitching motion on the nine hull variations can be seen in Fig. 15.

Based on the results of the seakeeping analysis of the pitching motion with a wave angle of 180°, the round bottom 3 ship model had the lowest motion response compared to the other models at a frequency of 4.63 rad/s. In contrast, the shallow vee 1 model had the highest maximum motion response value compared to the other models at a frequency of 5.44 rad/s. The hull types with the most insufficient pitching motion response were shallow vee, deep vee, and round bottom. Based on the pitching RAO of the nine ship variations, wave superposition did not occur where the ship did not receive more than one wave simultaneously, so the boat tended to be more stable. A recapitulation of the seakeeping analysis results can be seen in Table IX.

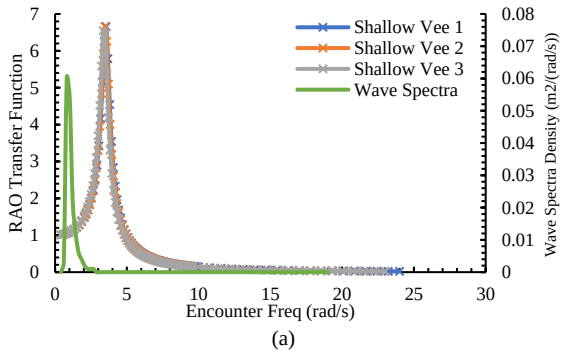

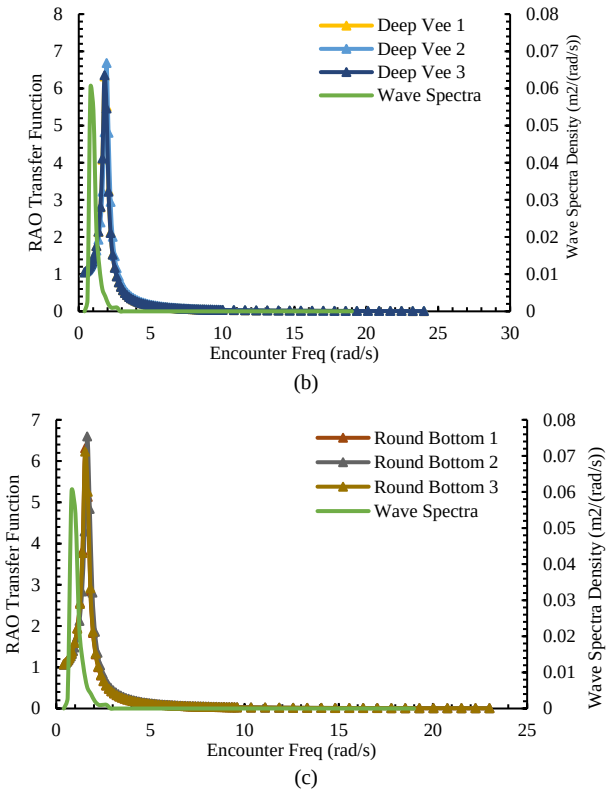

Fig. 15. RAO pitching motion, (a) shallow vee hull, (b) deep vee hull, (c) round bottom hull.

As leisure boats are used for tourism on water, comfort is one of the important aspects that must be considered in their design. Motion sickness incidence is a parameter of passenger comfort level when sailing [38]. This study conducted an MSI analysis when the ship sailed at 30 kts with a wave angle of 135 deg which can be seen in Fig. 16.

TABLE IX. RECAPITULATIONS OF THE SEAKEEPING RESULTS

Ship	Heaving (m/m)	Rolling (rad/rad)	Pitching (rad/rad)
Shallow vee 1	1.002	6.657	4.087
Shallow vee 2	1.000	6.662	4.174
Shallow vee 3	1.000	6.548	4.316
Deep vee 1	1.001	6.322	4.303
Deep vee 2	1.001	6.682	4.273
Deep vee 3	1.001	6.354	4.484
Round bottom 1	1.000	6.310	5.138
Round bottom 2	1.000	6.595	5.067
Round bottom 3	1.000	6.226	5.138

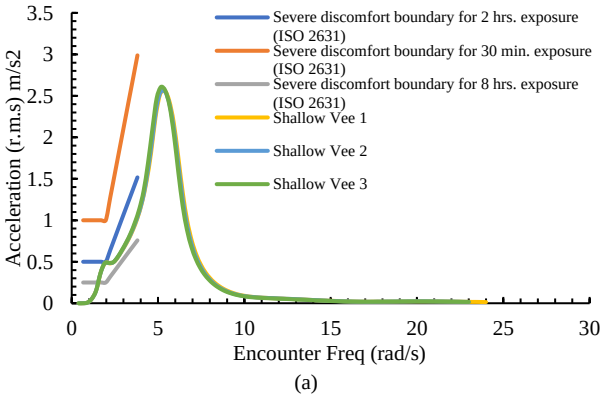

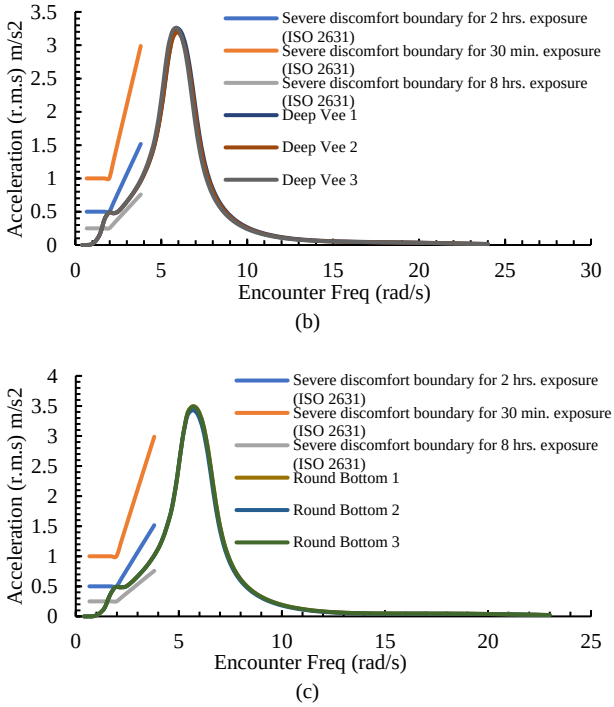

Fig. 16. MSI chart, (a) shallow vee hull, (b) deep vee hull, (c) round bottom hull.

Based on the charts above, the nine hull variation models can be considered to have a good level of comfort, because passengers will only experience symptoms of seasickness after sailing on the ship for more than 2 h. However, this study only used a variation of the leisure boat model with an LOA of 7 m, where boats of this dimensions generally only sail for a short time.

In the seakeeping analysis, the probability of slamming and deck wetness should be reduced, because slamming can damage the overall strength of the ship's structure, and deck wetness can reduce the comfort of passengers who are sailing due to splashing water. The slamming and deck wetness analysis was conducted when the ship sailed at 10 kts with 135 deg waves. The results of the slamming and deck wetness analysis can be seen in Table X.

TABLE X. PROBABILITY OF SLAMMING AND DECK WETNESS OF THE NINE HULL VARIATIONS

Model	Criteria	
	Slamming (MII/H)	Deck Wetness (MII/H)
Shallow vee 1	1.29	0.29
Shallow vee 2	1.25	0.10
Shallow vee 3	1.10	0.29
Deep vee 1	0.72	0.06
Deep vee 2	0.79	0.06
Deep vee 3	0.85	0.05
Round bottom 1	0.62	0.44
Round bottom 2	0.47	0.45
Round bottom 3	0.62	0.43

Based on the data in Table IX, the round-bottom hull-type variation with dimensions Variation 2 had the lowest probability of slamming with a value of 0.47 MII/H, and the lowest probability of deck wetness was obtained by the deep vee hull-type variation with dimensions Variation 3 with a value of 0.05 (MII/H), which means that the

probability of slamming and deck wetness is less than once per hour. The shallow vee 1 hull-type variation with dimensions Variation 1 had the highest probability of slamming with a value of 1.29 MII/H, and the highest probability of deck wetness was obtained by the round-bottom hull-type variation with dimensions Variation 2 with a value of 0.45 MII/H, which means that the probability of slamming occurring is more than once per hour.

D. Sensitivity Analysis

In the sensitivity analysis, we used a regression approach to obtain the coefficient value, standard error, *p*-values, R^2, and significant F to determine the effect of the dimensions variations and hull-type variations in this study; in the hull-type variation, the coefficient block value and simulation results were used as the input data, while in the dimensions variations, the displacement volume value and simulation results were used as the input data for the sensitivity analysis. The greater the R square value, the greater the variable significantly influences the hydrodynamic criteria. The indicator coefficient signifies the number of changes in x that must be multiplied to produce a corresponding average change in *y* or the number of changes in y for each unit increase in *x*. In this way, it represents the degree of the upward or downward slope of the line. A higher coefficient value implies a smaller influence of the variation on the outcome.

The regression standard error represents the average distance of the observed values from the regression line. Nevertheless, it tells how wrong the regression model is on average using the units of the response variable, so the higher the value of the standard error, the less significant the effect of changing the variation on the final result. The *p*-values indicator shows the probability of observing the coefficient values; the more significant the *p*-value, the smaller the effect of the variation on the final result. The significant F in regression is a test of the linear regression model in providing a better fit to the data set than a model without predictor variables. The smaller the significant F-value, the greater the effect of the variation on the final result. The sensitivity analysis results of the hydrodynamic resistance criterion can be seen in Table XI and Fig. 17.

TABLE XI. SENSITIVITY ANALYSIS RESULT: RESISTANCE

Indicator		Variations	
		Hull Type	Hull Dimensions
Resistance	Coefficient	–9.4049	9.9843
	Standard Error	2.0769	0.8927
	p-values	0.6193	0.0007
	R^2	0.0372	0.8221
	Significant F	0.6193	0.0007

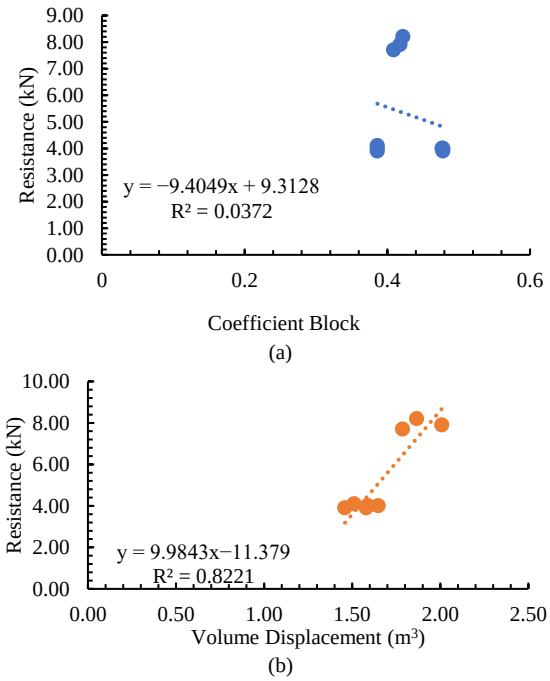

Fig. 17. Sensitivity analysis of the resistance parameter: (a) hull type; (b) dimension.

Based on the data in Table XI and Fig. 17, the dimensions variation had a greater significant influence because it had a more considerable R^2 value and a smaller F significance. In addition, the larger values of the coefficient, standard error, and *p*-value indicate that the hull-type variation had a minor effect on the final result. The sensitivity analysis results of the hydrodynamic stability criterion can be seen in Table XII and Fig. 18.

TABLE XII. RESULT OF THE SENSITIVITY ANALYSIS: STABILITY

Indicator		Variations	
		Hull Type	Hull Dimensions
Stability	Coefficient	–70.0643	7.2113
	Standard Error	1.7469	3.2201
	p-values	0.0025	0.2922
	R^2	0.7517	0.1563
	Significant F	0.0025	0.2922

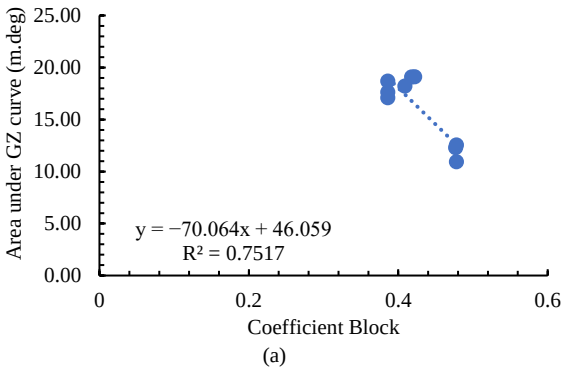

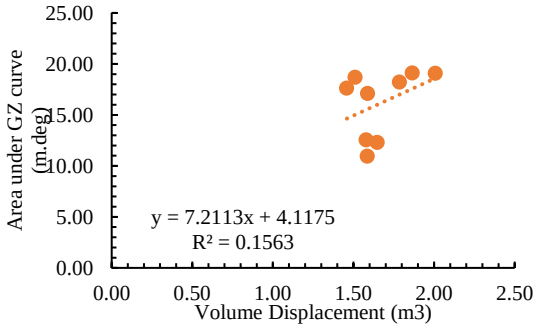

(b)

Fig. 18. Chart of the sensitivity analysis of the stability parameter: (a) hull type; (b) dimension.

Based on the data in Table XIII and Fig. 19, the hull-type variation had a more significant effect, because it had a more considerable R^2 value and a smaller F significance. In addition, the larger values of the coefficient, standard error, and *p*-value indicate that the dimensions variation had a minor effect on the final result. The sensitivity analysis results of the seakeeping heaving motion can be seen in Table XIII and Fig. 19.

TABLE XIII RESULT OF THE SENSITIVITY ANALYSIS: HEAVING MOTION

Indicator		Variations	
		Hull Type	Hull Dimensions
Heaving	Coefficient	8.3412	–1.6002
	Standard Error	0.3731	0.4190
	p-values	0.0372	0.0932
	R^2	0.4847	0.3502
	Significant F	0.0372	0.0932

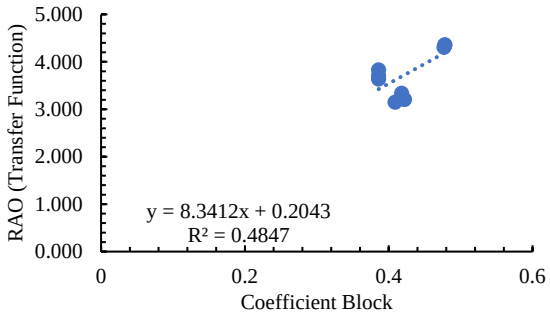

(a)

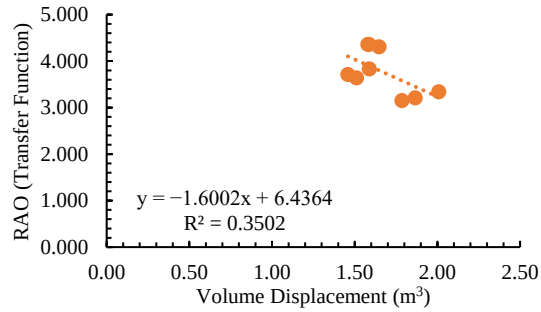

(b)

Fig. 19. Chart of the sensitivity analysis of the heaving motion parameter: (a) hull type; (b) dimension.

Based on the data in Table XIII and Fig. 19, the hull-type variation had a more significant effect, because it had a larger R^2 value and a smaller F significance. In addition, the larger values of the coefficient, standard error, and *p*-value indicate that the dimensions variation had a minor effect on the final result. The sensitivity analysis results of the seakeeping—rolling motion hydrodynamics criterion can be seen in Table XIV and Fig. 20.

TABLE XIV. RESULTS OF THE SENSITIVITY ANALYSIS: ROLLING MOTION

Indicator		Variations	
		Hull Type	Hull Dimensions
Rolling	Coefficient	–0.9215	0.3403
	Standard Error	0.1294	0.1186
	p-values	0.4407	0.1878
	R^2	0.0871	0.2333
	Significant F	0.4407	0.1878

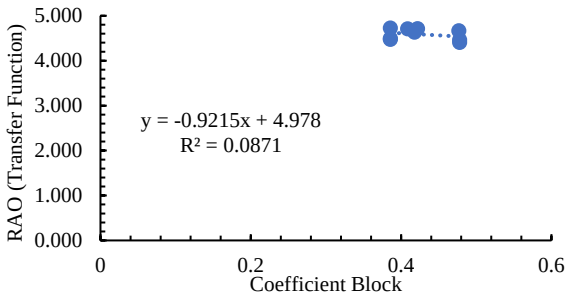

(a)

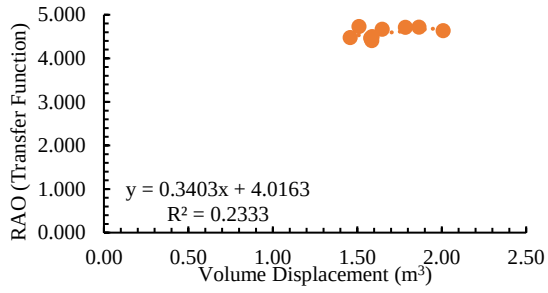

(b)

Fig. 20. Sensitivity analysis of the rolling motion: (a) hull type; (b) dimension.

Based on the data in Table XIV and Fig. 20, the dimensions variation had a more significant influence, because it had a more considerable R^2 value and a smaller F significance. In addition, the larger values of the coefficient, standard error, and *p*-value indicate that the hull-type variation had a minor effect on the final result. The sensitivity analysis results of the seakeeping—pitching motion hydrodynamics criterion can be seen in Table XV and Fig. 21.

TABLE XV. RESULT OF THE SENSITIVITY ANALYSIS: PITCHING MOTION

Indicator		Variations	
		Hull Type	Hull Dimensions
Pitching	Coefficient	6.5957	–0.7445
	Standard Error	0.1851	0.3093
	p-values	0.0046	0.2605
	R^2	0.7050	0.1763
	Significant F	0.0046	0.2605

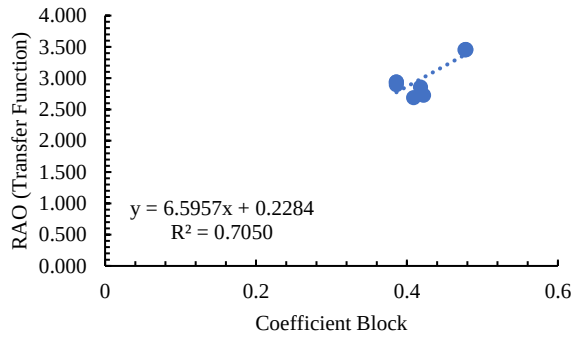

(a)

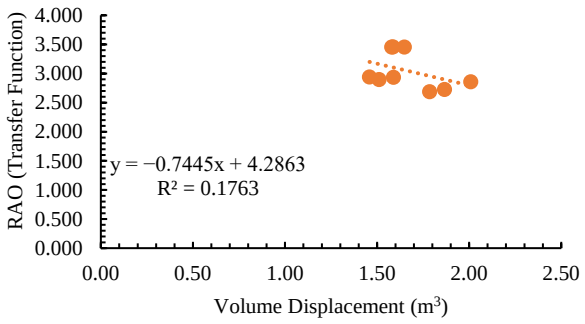

(b)

Fig. 21. Sensitivity analysis of the pitching motion: (a) hull type; (b) dimension.

Based on the data in Table XVI and Fig. 22, the hull-type variation had a more significant effect, because it had a more considerable R^2 value and a smaller F significant. In addition, the larger values of the coefficient, standard error, and *p*-value indicate that the dimensions variation had a minor effect on the final result. The sensitivity analysis results of the Motion Sickness Incidence (MSI) criterion can be seen in Table XVI and Fig. 22.

TABLE XVI. SENSITIVITY ANALYSIS RESULT: MSI

Indicator		Variations	
		Hull Type	Hull Dimensions
MSI	Coefficient	7.2033	3.9330
	Standard Error	0.7592	0.3201
	p-values	0.3122	0.0004
	R^2	0.1449	0.8479
	Significant F	0.3122	0.0004

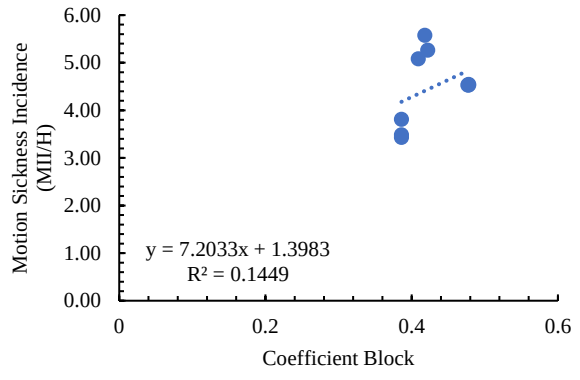

(a)

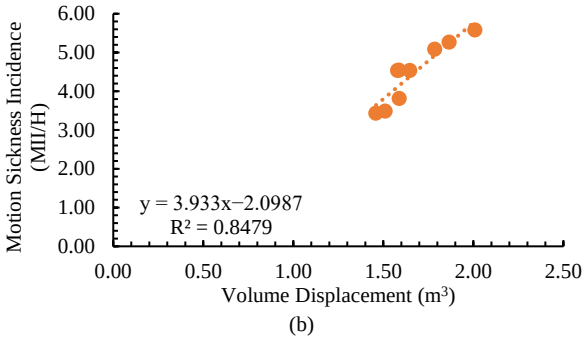

(b)

Fig. 22. Sensitivity analysis of the MSI: (a) hull type; (b) dimension.

Based on the data in Table XVI and Fig. 22, the dimensions variation had a more significant influence, because it had a more considerable R^2 value and a smaller F significance. In addition, the larger values of the coefficient, standard error, and *p*-value indicate that the hull-type variation had a minor effect on the final result. The sensitivity analysis results of the slamming criterion can be seen in Table XVII and Fig. 23.

Based on the data in Table XVII and Fig. 23, the dimensions variation had a more significant influence, because it had a more considerable R^2 value and a smaller F significance. In addition, the larger values of the coefficient, standard error, and *p*-value indicate that the hull-type variation had a minor effect on the final result. The sensitivity analysis results of the deck wetness criterion can be seen in Table XVIII and Fig. 24.

Based on the data in Table XVIII and Fig. 24, the hull-type variation had a more significant effect because it had a more considerable R^2 value and a smaller F significance. In addition, the larger values of coefficient, standard error, and *p*-values indicate that the dimensions variation had a minor effect on the final result.

TABLE XVII. SENSITIVITY ANALYSIS RESULT: SLAMMING

Indicator		Variations	
		Hull Type	Hull Dimension
Slamming	Coefficient	−3.5393	1.1599
	Standard Error	0.2732	0.2203
	p-Values	0.1806	0.0316
	R^2	0.2400	0.5061
	Significant F	0.1806	0.0316

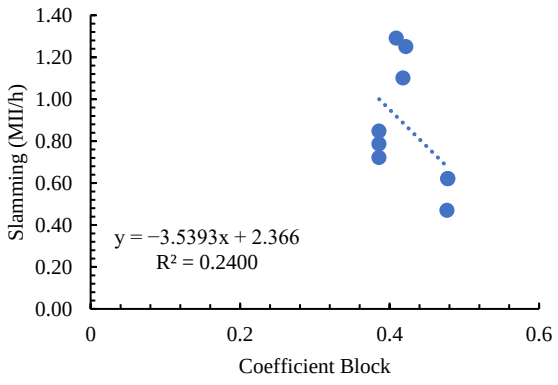

(a)

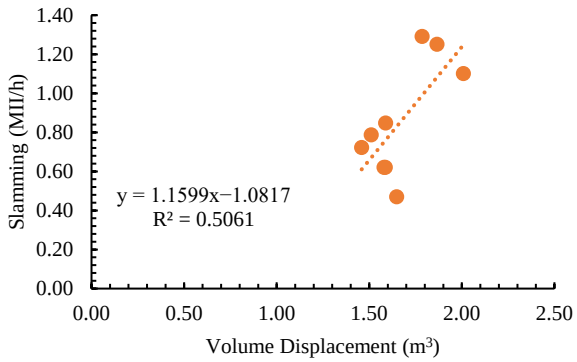

(b)

Fig. 23. Sensitivity analysis of the slamming: (a) hull type; (b) dimension.

TABLE XVIII. SENSITIVITY ANALYSIS RESULT: DECK WETNESS

Indicator		Variations	
		Hull Type	Hull Dimensions
Deck Wetness	Coefficient	3.9279	0.1358
	Standard Error	0.0731	0.1836
	p-values	0.0005	0.7179
	R^2	0.8445	0.0198
	Significant F	0.0005	0.7179

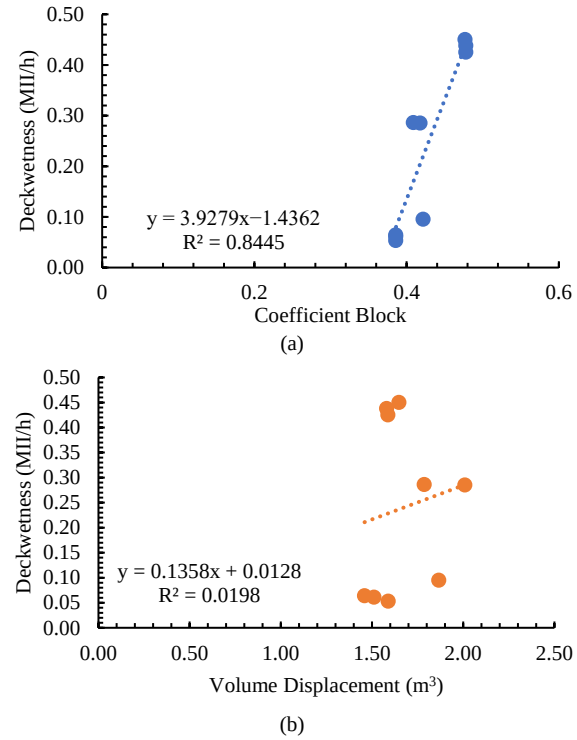

(a)

(b)

Fig. 24. Sensitivity analysis of the deck wetness: (a) hull type; (b) dimension.

Multiattribute Decision-Making (MADM)

After all analysis were completed, the last stage of this study was to select the best design with the multiattribute decision-making method based on its hydrodynamic characteristics. In this study, resistance only had a score of 5% because a leisure boat is a ship intended for traveling, so speed is not the most critical factor. Stability and slamming had a score of 10%, because the stability of leisure boats has a more crucial role, and the probability of slamming is considered critical so that the safety of passengers when sailing is maintained. The criteria of heaving, rolling, pitching, MSI, and deck wetness had a score of 15%, because these criteria have the most crucial roles so that passenger comfort when sailing is maintained. The summarized scores are presented in Table XIX.

TABLE XIX. DESIGNATED SCORE OF THE MAIN CRITERIA

Parameter	Criteria	Weight (%)
Resistance	C1	5
Stability	C2	10
Heaving	C3	15
Rolling	C4	15
Pitching	C5	15
MSI	C6	15
Slamming	C7	10
Deck Wetness	C8	15

Resistance was analyzed when the ship operated at 30 kts, and stability was based on the area under the GZ curve. In the seakeeping parameters, the value taken was the highest value of the RAO in each movement, including heaving, rolling, and pitching. The model variation with the highest score was the best model in this study. Data from the nine variation models for the MADM analysis can be seen in Table XX.

The next stage was the data normalization stage to avoid data anomalies. In criteria C1 and C3–C8, minor data were selected because the smaller the resistance value and the value of RAO's peak point, the smaller the ship design. However, in criteria C2, the largest value was used because the larger the area under GZ curve, the better the ship design. The normalization data for the nine hull variations can be seen in Table XXI.

After the data normalization was carried out, calculations could be made with scores for each criterion. The model with the highest final score is the model with the best design among all of the models. The results of the total values of the nine variation models can be seen in Table XXII.

After determining the total score of the nine variation models, the next step was to rank them to determine the best model with the highest final score. The results of the ranking of the nine variation models can be seen in Table XXIII.

Based on the data shown in Table XXII, it can be found that the deep vee 1 model, which is the result of a regression approach with displacement and LOA locks, is the model that has the best hydrodynamic characteristics, with a final score of 0.910. Meanwhile, the model with the worst hydrodynamic characteristics is the round bottom 3, which is also the result of a regression approach with displacement and draft locks, with a final score of 0.691.

TABLE XX. PARAMETER VALUES OF THE NINE MODEL VARIATIONS

Model	Criteria							
	C1	C2	C3	C4	C5	C6	C7	C8
S.V. 1	7.700	18.200	3.146	4.707	2.686	5.080	1.290	0.286
S.V. 2	8.200	19.100	3.205	4.711	2.723	5.262	1.250	0.095
S.V. 3	7.900	19.070	3.334	4.630	2.855	5.575	1.100	0.285
D.V. 1	3.900	17.610	3.707	4.470	2.937	3.431	0.721	0.064
D.V. 2	4.100	18.670	3.636	4.725	2.893	3.485	0.786	0.061
D.V. 3	4.000	17.080	3.829	4.493	2.933	3.810	0.847	0.053
R.B. 1	3.900	12.540	4.354	4.462	3.451	4.530	0.620	0.438
R.B. 2	4.000	12.280	4.304	4.663	3.451	4.530	0.469	0.450
R.B. 3	4.000	10.930	4.354	4.403	3.454	4.542	0.620	0.425

TABLE XXI. NORMALIZED MADM RECAPITULATIONS

Model	Criteria							
	C1	C2	C3	C4	C5	C6	C7	C8
S.V. 1	0.506	0.953	1.001	0.935	1.001	0.675	0.364	0.210
S.V. 2	0.476	1.000	0.983	0.934	0.988	0.652	0.376	0.632
S.V. 3	0.494	0.998	0.945	0.950	0.942	0.615	0.427	0.211
D.V. 1	1.000	0.922	0.850	0.984	0.916	1.000	0.652	0.938
D.V. 2	0.951	0.977	0.866	0.931	0.930	0.984	0.598	0.984
D.V. 3	0.975	0.894	0.823	0.979	0.917	0.900	0.555	1.132
R.B. 1	1.000	0.657	0.723	0.986	0.779	0.757	0.758	0.137
R.B. 2	0.975	0.643	0.732	0.944	0.779	0.757	1.002	0.133
R.B. 3	0.975	0.572	0.723	0.999	0.779	0.755	0.758	0.141

TABLE XXII. TOTAL VALUES OF THE ASSESSED MODELS

Model	Criteria							
	C1	C2	C3	C4	C5	C6	C7	C8
S.V. 1	0.025	0.095	0.150	0.140	0.150	0.101	0.036	0.031
S.V. 2	0.024	0.100	0.147	0.140	0.148	0.098	0.038	0.095
S.V. 3	0.025	0.100	0.142	0.143	0.141	0.092	0.043	0.032
D.V. 1	0.050	0.092	0.127	0.148	0.137	0.150	0.065	0.141
D.V. 2	0.048	0.098	0.130	0.140	0.139	0.148	0.060	0.148
D.V. 3	0.049	0.089	0.123	0.147	0.138	0.135	0.055	0.170
R.B. 1	0.050	0.066	0.109	0.148	0.117	0.114	0.076	0.021
R.B. 2	0.049	0.064	0.110	0.142	0.117	0.114	0.100	0.020
R.B. 3	0.049	0.057	0.109	0.150	0.117	0.113	0.076	0.021

TABLE XXIII. MADM RANKING RESULTS

Ranking	Model	Score
1	D.V. 1 (Deep vee 1)	0.910
2	DV. 2 (Deep vee 2)	0.909
3	D.V. 3 (Deep vee 3)	0.906
4	S.V. 2 (Shallow vee 2)	0.790
5	S.V. 1 (Shallow vee 1)	0.730
6	S.V.3 (Shallow vee 3)	0.717
7	R.B. 2 (Round bottom 2)	0.715
8	R.B. 1 (Round bottom 1)	0.699
9	R.B. 3 (Round bottom 3)	0.691

V. CONCLUSIONS

In this study, hydrodynamic criteria, including resistance, stability, and seakeeping, were analyzed with two different variation parameters: hull-type variation and hull dimensions variation. In this study, the following conclusions were obtained.

In resistance analysis, shallow vee hull-type exhibited the highest resistance, while the deep vee hull-type had the lowest. It can be found that hull dimensions had a more significant impact on resistance than hull-type variation. In stability criterion, deep vee hull-type demonstrated the highest GZ arm value. Hull shape had a more significant effect on stability than hull dimensions.

Moreover, hull type influenced heaving, rolling, and pitching motions, with round bottom having the highest RAO values. Shallow vee hull-type had the lowest MSI values, indicating greater comfort, while round-bottom had the highest discomfort. Dimensions variation had a greater impact on rolling motion, while hull-type had a more significant effect on heaving and pitching motions. In addition, round bottom had the lowest probability of slamming, while shallow vee had the highest but deep vee had the lowest probability of deck wetness, while round bottom had the highest.

Multiattribute Decision-Making (MADM) shows deep vee variation was identified as the best model, followed by shallow vee and round-bottom models. Among dimension

variations, Variation 2 (displacement and draft regression) was considered the best.

NOMENCLATURES

Cf:	Coefficient of frictional resistance
Cv:	Coefficient of viscous resistance
Fn:	Froude number
G:	Center of gravity
g:	Gravity acceleration (m/s^2)
GZ:	Distance of point G to Z (m)
K:	Turbulence kinetic energy (m^2/s^2)
L:	Length of waterline (m)
m4:	Spectral moment of the ship
Rf:	Frictional resistance (N)
Rn:	Reynold number
Rv:	Viscous resistance (N)
Rw:	Wave resistance (N)
S:	Wetted area (m^2)
V:	Displacement volume (m^3)
v:	Speed (m/s)

CONFLICT OF INTEREST

The authors declare no conflict of interest.

AUTHOR CONTRIBUTIONS

Conceptualization, A.R.P., T.M. T.T. and J.H.C.; methodology, W.W. and N.M.; software, A.R.Y. and E.M.M.; validation, A.R.Y. and E.M.M.; formal analysis, A.R.Y., E.M.M. and H.D.; investigation, A.R.Y., E.M.M. and H.D; resources, A.R.P.; data curation, N.M. and T.T.; writing—original draft preparation, N.M., A.R.P. and T.T.; writing—review and editing, A.R.P., T.M. and T.T.; visualization, A.R.Y. and E.M.M.; supervision, N.M., A.R.P. and J.H.C.; project administration, N.M., A.R.P. and W.W.; funding acquisition, A.R.P., T.T. and W.W. All authors have read and agreed to the published version of the manuscript.

FUNDING

This work was supported by the RKAT PTNBH Universitas Sebelas Maret Year 2022, under the Research Scheme of "Penelitian Disertasi Doktor" (PDD-UNS), with research grant/contract no. 254/UN27.22/PT.01.03/2022. The support is gratefully acknowledged by the authors.

ACKNOWLEDGMENT

The authors would like to express gratitude to the Laboratory of Design, Faculty of Mechanical Engineering at Universitas Sebelas Maret for providing research facilities and assistance with numerical analysis.

REFERENCES

[1] A. Nugroho, O. S. Suharyo, and A. Rahman, "The development of Indonesian maritime potential and prospects towards a world maritime axis," in *Proc. STTAL Postgraduate-International Conference*, 2020, vol. 4, no. 1.

[2] A. Y. Iriani, "Tourism development strategy based on indigenous people's preferences: A case study in Raja Ampat," *J. Masy. Bud.*, vol. 27, pp. 271–292. 2019. https://doi.org/10.14203/jmb.v21i3.731

[3] A. Lumaksono, D. S. Priyarsono, Kuntjoro, and R. Heriawan, "The economic impact of international tourism on the Indonesian economy," *For. Pascasarj.*, vol. 35, pp. 53–68, 2012.

[4] N. S. Nengsih, "Application of sustainable development indicators in coastal areas in marine biodiversity for the welfare of society," *J. Ilmu. Sos. Ilmu. Pol.*, vol. 1, pp. 151–162, 2020. https://doi.org/10.56552/jisipol.v1i2.17

[5] BLUD UPTD. (2023). Kawasan konservasi perairan di raja ampat. BLUD UPTD raja ampat archipelago marine protected area. [Online]. Available: https://kkprajaampat.com/

[6] Papilaya, L. Renoldy, B. Paulus, and P. N. Victor, "Carrying capacity of diving tourism in dampier strait marine conservation area—District of raja ampat," *IOP Conference Series: Earth and Environmental Science*, vol. 246, no. 1, 2019.

[7] K. Kurniawan, "The silence of a small island: travel notes on one of the islands in Raja Ampat," *Warta Pariwisata*, vol. 18, no. 1, pp. 14–15, 2020. https://doi.org/10.5614/wpar.2020.18.1.07

[8] I. N. S. Arida, "Tri Ning Tri ecotourism dynamics in Bali: Problems and strategies for the development of three types of Bali eco-tourism," *Jurnal Kawistara*, vol. 4, pp. 111–224, 2015. https://doi.org/10.22146/kawistara.5666

[9] M. Anjasomoro. (2023). Underwater tourism in Raja Ampat Waters. [Online]. Available: https://hardrockfm.com/wisata-bawah-laut-di-perairan-raja-ampat/

[10] A. R. Prabowo, E. Martono, T. Muttaqie, T. Tuswan, and D. M. Bae, "Effect of hull design variations on the resistance profile and wave pattern: A case study of the patrol boat vessel," *J. Eng. Sci. Technol.*, vol. 17, pp. 106–126, 2022.

[11] R. I. Julianto, A. R. Prabowo, N. Muhayat, T. Putranto, and R. Adiputra, "Investigation of hull design to quantify resistance criteria using Holtrop's regression-based method and Savitsky's mathematical model: A study case of fishing vessels," *J. Eng. Sci. Technol.*, vol. 16, pp. 1426–1443, 2021.

[12] R. A. Febrianto, S. Hadi, R. L. L. Hidayat, D. M. Bae, B. Cao,and A. R. Prabowo, "Implementation of Fluid-Structure Interaction (FSI) in marine design: Calculation review on hull structures," in *Proc. AIP Conf.*, 2023, vol. 2674, issue 1. https://doi.org/10.1063/5.0114201

[13] R. A. Febrianto, A. R. Prabowo, S. J. Baek, and R. Adiputra, "Analysis of monohull design characteristics as supporting vessel for the COVID-19 medical treatment and logistic," *Transport. Res. Proc.*, vol. 55, pp. 699–706, 2021. https://doi.org/10.1016/j.trpro.2021.07.038

[14] M. Yusvika, A. R. Prabowo, D. D. D. P. Tjahjana, and J. M. Sohn, "Cavitation prediction of ship propeller based on temperature and fluid properties of water," *J. Mar. Sci. Eng.*, vol. 8, no. 465, 2020, https://doi.org/10.3390/jmse8060465

[15] S.Jeong and H. Kim, "Development of an efficient hull form design exploration framework," *Math. Prob. Eng.*, 838354, 2013. https://doi.org/10.1155/2013/838354

[16] J. H. Ang, C. Goh, and Y. Li, "Hull form design optimization for improved efficiency and hydrodynamic performance of "ship-shaped" offshore vessels," in *Proc. International Conference on Computer Applications in Shipbuilding*, 2015, pp. 71–80.

[17] R. I. Julianto, T. Muttaqie, R. Adiputra, S. Hadi, R. L. L. G. Hidajat, and A. R. Prabowo, "Hydrodynamic and structural investigations of catamaran design," *Proc. Struct. Integ.*, vol. 27, pp. 93–100, 2020. https://doi.org/10.1016/j.prostr.2020.07.013

[18] T. Rahmaji, A. R. Prabowo, T. Tuswan, T. Muttaqie, N. Muhayat, and S. J. Baek, "Design of fast patrol boat for improving resistance, stability, and seakeeping performance," *Des.*, vol. 17, no. 105, 2022. https://doi.org/10.3390/designs6060105

[19] S. Radfar, A. aherkhani, and R. Ahi, "Standardization of the main dimensions of design container ships in ports—A case study," *World J. Eng. Technol.*, vol. 5, pp. 51–61, 2017. https://doi.org/10.4236/wjet.2017.54B006

[20] H. O. Kristensen, "Determination of regression formulas for main dimensions of tankers and bulk carriers based on IHS fairplay data," *Technical Report for Project*, no. 56, 2012.

[21] O. Yurdakul, G. N. Kuçuksu, A. Z. Saydam, and M. S. Çalışal, "A decision-making process for the selection of better ship main dimensions by a Pareto frontier solution," *Ocean Eng.*, vol. 239, 109908, 2021. https://doi.org/10.1016/j.oceaneng.2021.109908

[22] Y. S. Yang, C. K. Park, K. H. Lee, and J. C. Suh, "A study on the preliminary ship design method using deterministic approach and probabilistic approach including hull form," *Struct. Multidiscip. Optim.*, vol. 33, pp. 529–539, 2006. https://doi.org/10.1007/s00158-006-0063-5
[23] R. Campbell, M. Terziev, T. Tezdogan, and A. Incecik, "Computational fluid dynamics predictions of draught and trim variations on ship resistance in confined waters," *Appl. Ocean Res.*, vol. 126, 103301, 2022. https://doi.org/10.1016/j.apor.2022.103301
[24] A. F. Molland, S. R. Turnock, and D. A. Hudson, *Ship Resistance and Propulsion*, Cambridge University Press, 2017.
[25] Q. Zeng, R. Hekkenberg, and C. Thill, "On the viscous resistance of ships sailing in shallow water," *Ocean Eng.*, vol. 190, 106434, 2019. https://doi.org/10.1016/j.oceaneng.2019.106434
[26] M. S. Tarafder and A. R. Saaki, "Computation of resistance of high-speed planing craft using Savitsky's theory," in *Proc. AIP Conf.*, 1980, 040006, vol. 2018. https://doi.org/10.1063/1.5044316
[27] E. Sancak and F. Çakici, "Determination of the optimum trim angle of a planing hull for minimum drag using Savitsky method," *Gemi ve Deniz Teknolojisi*, vol. 220, pp. 43–53, 2021. https://doi.org/10.54926/gdt.951371
[28] D. B. Uhls, *Does the Fast Patrol Boat Have a Future in the Navy?* United States Army Command and General Staff College: Kansas, United States, 2002.
[29] A. R. Prabowo, R. A. Febrianto, T. Tuswan, and D. D. D. P. Tjahjana, "Performance evaluation on the designed V-shaped monohull ship models," *J. Appl. Eng. Sci.*, vol. 20, pp. 610–624, 2022.
[30] J. Holtrop and G. G. J. Mennen, "An approximate power prediction method," *International Shipbuilding Progress*, vol. 29, no. 335, pp. 166–170, 1982.
[31] B. Adrian and P. R. Lopez, *Ship Hydrostatics and Stability*, 2nd ed., Butterworth-Heinemann, 2014.
[32] C. B. Barrass and D. R. Derrett, *Ship Stability for Masters and Mates*, 6th ed., Butterworth-Heinemann, 2006.
[33] P. Ruponen, *Principles of Ship Buoyancy and Stability*, Aalto University Publication Series: Aalto, Finland, 2021.
[34] A. Afriantoni, R. Romadhoni, and B. Santoso, "Study on the stability of high-speed craft with step hull angle variations," *IOP Conf. Series: Earth and Environ. Sci.*, vol. 430, 012040, 2020. https:/doi.org/10.1088/1755-1315/430/1/012040
[35] H. Carvalho, R. Ridwan, S. Sudarno, A. R. Prabowo, D. M. Bae, and N. Huda, "Failure criteria in crashworthiness analysis of ship collision and grounding using FEA: Milestone and development," *Mek. Majalah Ilmiah Mek.*, vol. 22, pp. 30–39, 2023. https://doi.org/10.20961/mekanika.v22i1.70959
[36] N. Nurhasanah, B. Santoso, R. Romadhoni, and P. Nasutioni, "Seakeeping analysis of hull rounded design with multi-chine model on fishing vessel," *IOP Conf. Series: Earth Environ. Sci.*, vol. 430, 012041. 2020. https://doi.org/10.1088/1755-1315/430/1/012041
[37] R. Bhattacharyya, *Dynamics of Marine Vehicles*, John Wiley & Sons, 1978.
[38] I. Ibinabo and D. T. Tamunodukobipi, "Determination of the response amplitude operator(s) of an FPSO," *Eng.*, vol. 11, pp. 541–556, 2019. https://doi.org/10.4236/eng.2019.119038
[39] A. Scamardella and V. Piscopo, "Passenger ship seakeeping optimization by the overall motion sickness incidence," *Ocean Eng.*, vol. 76, pp. 86–97, 2014. https://doi.org/10.1016/j.oceaneng.2013.12.005
[40] V. M. Nguyen, M. Jeon, and H. K. Yoon, "Study on the optimal weather routing of a ship considering parametric rolling, slamming, and deck wetness," in *Proc. International Symposium on Practical Design of Ships and Other Floating Structures*, Copenhagen, Denmark, 2016.
[41] J. Junaidi, M. Fajri, and Y. Ristawan, "The sensitivity analysis of multiple linear regression models uses a Bayesian approach (prior normal distribution)," *J. Data Anal.*, vol. 3, no. 1, pp. 1–12, 2021.
[42] Z. Xu, "On multi-period multi-attribute decision making," *Knowl. Based Syst.*, vol. 21, pp. 164–171, 2008. https://doi.org/10.1016/j.knosys.2007.05.007
[43] S. H. Zanakis, A. Solomon, N. Wishart, and S. Dublish, "Multi-attribute decision making: A simulation comparison of select methods," *Eur. J. Operat. Res.*, vol. 107, pp. 507–529. 1998. https://doi.org/10.1016/S0377-2217(97)00147-1
[44] H. Diatmaja, A. R. Prabowo, N. Muhayat, T. Tuswan, and T. Putranto, "Fast ship prototype design simulation with fin stabilizer on hydrodynamic characteristics for ship realization planning," *IOP Conf. Series: Earth Environ. Sci.*, 1166, 012047, 2023. https://doi.org/10.1088/1755-1315/1166/1/012047
[45] K. Bhawsinka, "Maneuvering simulation of displacement type ship and planing hull," Memorial University of Newfoundland: Newfoundland and Labrador, Canada, 2012.
[46] H. Nubli, F. S. Utomo, H. Diatmaja, A. R. Prabowo, U. Ubaidillah, D. D. Susilo, and F. B. Laksono, "Design of the Bengawan Unmanned Vehicle (UV) roboboat: Mandakini Neo. Mek," *Applied and Engineering Mechanics—A Scientific Journal*, vol. 21, pp. 64–74, 2022. https://doi.org/10.20961/mekanika.v21i2.61624
[47] M. Yusvika, A. Fajri, T. Tuswan, A. R. Prabowo, S. Hadi, I. Yaningsih, T. Muttaqie, and F. B. Laksono, "Numerical prediction of cavitation phenomena on marine vessel: Effect of the water environment profile on the propulsion performance," *Open Eng.*, vol. 12, pp. 293–312, 2022. https://doi.org/10.1515/eng-2022-0034
[48] A. S. Pratama, A. R. Prabowo, T. Tuswan, R. Adiputra, N. Muhayat, B. Cao, S. Hadi, and I. Yaningsih, "Fast patrol boat hull design concepts on hydrodynamic performances and survivability evaluation," *J. Appl. Eng. Sci.*, vol. 21, pp. 501–531. 2023. https://doi.org/10.5937/jaes0-40698
[49] T. Rahmaji, A. R. Prabowo, N. Muhayat, T. Tuswan, and T. Putranto, "Effect of bilge keel variations on the designed fast patrol boats to hull resistance and stability behaviors," *IOP Conf. Series: Earth Environ. Sci.*, vol. 1166, 012048, 2023. https://doi.org/10.1088/1755-1315/1166/1/012048
[50] A. S. Pratama, A. R. Prabowo, N. Muhayat, T. Putranto, and T. Tuswan, "Analysis of hull performance on fast patrol boat with an extended study of survivability under damaged conditions," *IOP Conf. Series: Earth Environ. Sci.*, vol. 1166, 012046, 2023. https://doi.org/10.1088/1755-1315/1166/1/012046
[51] Y. Cheng, C. Xi, S. Dai, C. Ji, M. Collu, M. Li, Z. M. Yuan, and A. Incecik, "Wave energy extraction and hydroelastic response reduction of modular floating breakwaters as array wave energy converters integrated into a very large floating structure," *Applied Energy*, vol. 306, 117953, 2022.
[52] Y. Cheng, L. Fu, S. S. Dai, M. Collu, C. Y. Ji, Z. M. Yuan, and A. Incecik, "Experimental and numerical investigation of WEC-type floating breakwaters: A single-pontoon oscillating buoy and a dual-pontoon oscillating water column," *Coast Eng.*, vol. 177, 104188. 2022.
[53] Sea Temperature, "Sea temperature in Raja Ampat Islands in Indonesian Papua," 2023. Retrieved from https://www.seatemperatu.re/southeast-asia/indonesian-papua/raja-ampat-islands/